PERGAMON

International Journal of Heat and Mass Transfer 45 (2002) 451–459

International Journal of HEAT and MASS TRANSFER

www.elsevier.com/locate/ijhmt

Technical Note

Unsteady natural convection boundary-layer flow along a vertical isothermal plate in a linearly stratified fluid with $Pr > 1$

Wenxian Lin, S.W. Armfield *, P.L. Morgan

Department of Mechanical and Mechatronic Engineering, The University of Sydney, Sydney, NSW 2006, Australia

Received 18 September 2000; received in revised form 13 April 2001

Abstract

In this study, the unsteady natural convection boundary-layer flow along an impulsively heated vertical isothermal plate immersed in a stably stratified semi-infinite ambient fluid is explored using scaling analysis and direct numerical simulation. Scaling relations are obtained for the thermal and velocity boundary layer thicknesses, the boundary layer velocity, the development time and the Nusselt number, in terms of the Rayleigh and Prandtl numbers and the stratification parameter. The scaling results are validated using the numerical simulations.

1. Introduction

The transient response of a vertical natural convection flow, following from a suddenly imposed surface heating condition, has been investigated by many researchers. Most of these studies have been focused on obtaining similarity solutions under different surface heating conditions and ambient fluid temperatures. For example, Joshi and Gebhart [1] presented the general transient natural convection response arising from a sudden change of the level of energy input flux to a vertical surface element and compared their similarity solutions to the experimental results. The effects of a stable ambient thermal stratification on the stability and transition of a natural convection boundary-layer flow were studied by Jaluria and Gebhart [2]. Henkes and Hoogendoorn [3] presented all similarity solutions of the laminar natural convection boundary-layer equations for air.

An alternative means of studying the transient response of the vertical natural convection flow subject to a suddenly imposed surface heating conditions is to use the Patterson–Imberger scaling analysis [4] that was developed for natural convection flow in a differentially heated cavity with a uniform temperature. In this study, that scaling analysis procedure is used to provide scaling relations for the vertical natural convection flow in a linearly stratified ambient fluid, subject to a sudden temperature change on the vertical plate. Numerical results from direct simulation are then used to validate the scaling relations.

2. Formulation and scaling analysis

2.1. Governing equations

Under consideration is the unsteady natural convection boundary-layer flow along an isothermal vertical plate immersed in a linearly stratified semi-infinite fluid. The vertical plate, as sketched in Fig. 1, has a height of H. Initially the incompressible and viscous Newtonian fluid in the ambient is at rest and is linearly stratified, characterized by a constant temperature stratification number $S = \mathrm{d}T_a(Y)/\mathrm{d}Y$, where $T_a(Y)$ is the temperature of the local ambient fluid at the height Y. At time $t = 0$ the vertical plate is abruptly set to a temperature T_w and this temperature is maintained thereafter. A two-dimensional flow is assumed. It is also assumed that $\Delta T = T_w - T_a(0.5H)$ is fixed independent of the

* Corresponding author.

E-mail address: armfield@mech.eng.usyd.edu.au (S.W. Armfield).

0017-9310/02/$ - see front matter
PII: S0017-9310(01)00154-5

Nomenclature

$f(s)$	defined by (19)
g	acceleration due to gravity
H	height of plate
L	width of computational domain
$\overline{Nu}$	mean Nusselt number on the plate
p	$p = P/(\rho U_0^2)$
P	pressure
Pr	Prandtl number
Ra	Rayleigh number
t	time
T	temperature
T_a	local ambient temperature
T_f	fluctuating temperature
T_w	temperature imposed on the plate
u	$u = U/U_0$
u_b	horizontal velocity scale
U	horizontal velocity
U_0	$U_0 = \kappa Ra^{1/2}/H$
v	$v = V/V_0$
v_b	vertical velocity scale
$v_{b,t}$	vertical velocity scale during the developing stage
$v_{b,s}$	vertical velocity scale for fully developed stage
V	vertical velocity
x	$x = X/H$
X	horizontal coordinate
y	$y = Y/H$
y_s	termination height
Y	vertical coordinate
β	coefficient of thermal expansion
δ_b	boundary-layer thickness scale
$\delta_{b,t}$	thermal boundary-layer thickness scale during the developing stage
$\delta_{b,s}$	viscous boundary-layer thickness for fully developed stage
$\delta_{v,s}$	boundary-layer thickness scale for fully developed stage
θ	$\theta = (T - T_a(0.5H))/\Delta T$
θ_f	$\theta_f = (T_f - T_a(0.5H))/\Delta T$
θ_w	$\theta_w = (T_w - T_a(0.5H))/\Delta T$
κ	thermal diffusivity
ν	kinematic viscosity
ρ	density
τ	$\tau = t/(H/U_0)$
τ_b	time-scale
$\tau_{b,s}$	time-scale for fully developed stage
ΔT	$\Delta T = T_w - T_a(0.5H)$
Δx	first horizontal mesh size
Δy	first vertical mesh size
$\Delta\theta_f$	$\Delta\theta_f = 1 - (y - 0.5)s$
$\Delta\tau$	time-step

variables, S, Ra and Pr, where $T_a(0.5H)$ is the initial temperature of the local ambient fluid at height $Y = 0.5H$ and Ra and Pr are the Rayleigh number and Prandtl number, defined as

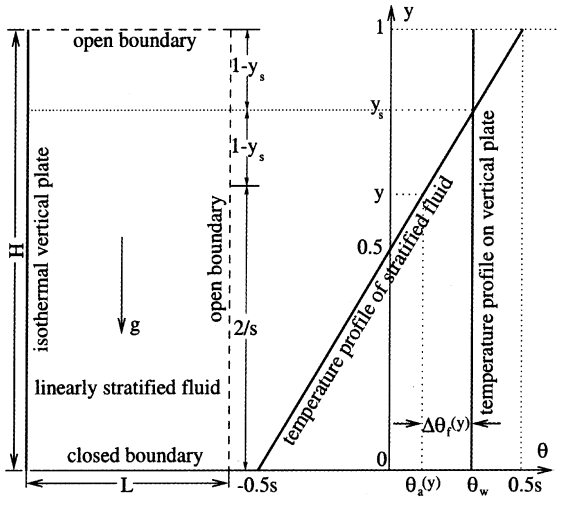

Fig. 1. Flow configuration and the initial temperature profiles for natural convection boundary-layer flows in a linearly stratified fluid.

$$Ra = \frac{g\beta\Delta T H^3}{\nu\kappa}, \quad Pr = \frac{\nu}{\kappa}, \tag{1}$$

where g is the acceleration due to gravity, ν, β and κ are the kinematic viscosity, coefficient of thermal expansion and thermal diffusivity of the fluid, respectively.

The governing equations are the Navier–Stokes equations plus the temperature transport equation, with the Boussinesq assumption allowing their incompressible forms to be used. If $T = T_f + T_a(Y)$ is used where T_f is the fluctuating temperature, the governing equations can be written in non-dimensional form as follows:

$$\frac{\partial u}{\partial x} + \frac{\partial v}{\partial y} = 0, \tag{2}$$

$$\frac{\partial u}{\partial \tau} + u\frac{\partial u}{\partial x} + v\frac{\partial u}{\partial y} = -\frac{\partial p}{\partial x} + \frac{Pr}{Ra^{1/2}}\left(\frac{\partial^2 u}{\partial x^2} + \frac{\partial^2 u}{\partial y^2}\right), \tag{3}$$

$$\frac{\partial v}{\partial \tau} + u\frac{\partial v}{\partial x} + v\frac{\partial v}{\partial y} = -\frac{\partial p}{\partial y} + \frac{Pr}{Ra^{1/2}}\left(\frac{\partial^2 v}{\partial x^2} + \frac{\partial^2 v}{\partial y^2}\right) + Pr\,\theta_f, \tag{4}$$

$$\frac{\partial \theta_f}{\partial \tau} + u\frac{\partial \theta_f}{\partial x} + v\frac{\partial \theta_f}{\partial y} + vs = \frac{1}{Ra^{1/2}}\left(\frac{\partial^2 \theta_f}{\partial x^2} + \frac{\partial^2 \theta_f}{\partial y^2}\right), \tag{5}$$

where u and v are the velocity components in the directions x and y, respectively, with x the horizontal

direction and y the vertical, τ is the time, θ is the temperature, p is the pressure and $s = \mathrm{d}\theta_a(y)/\mathrm{d}y = HS/\Delta T$ is the non-dimensional temperature stratification number, which is a constant when the environment is linearly stratified, where $\theta_a(y)$ is the non-dimensional form of $T_a(Y)$. The non-dimensional quantities are obtained as follows:

$$x = \frac{X}{H}, \quad y = \frac{Y}{H}, \quad u = \frac{U}{U_0}, \quad v = \frac{V}{U_0}, \quad \tau = \frac{t}{(H/U_0)}, \quad p = \frac{P}{\rho U_0^2}, \quad \theta = \frac{T - T_a(0.5H)}{\Delta T}, \tag{6}$$

where U and V are the horizontal and vertical components of velocity, P the pressure (including the hydrostatic pressure), and $U_0 = \kappa Ra^{1/2}/H$ which is the boundary layer velocity scale obtained by Patterson and Imberger [4] for natural convection flow in a cavity with differentially heated end walls.

The associated initial and boundary conditions are:

$$u = v = 0, \quad \theta_f = 0 \qquad \text{at all } x, y \quad \text{and} \quad \tau < 0, \tag{7}$$

and for $\tau \geqslant 0$

$$\begin{aligned}
&u = v = 0, \quad \theta_f = \theta_w - \theta_a(y) && \text{on } x = 0, \quad 0 \leqslant y \leqslant 1,\\
&\frac{\partial u}{\partial x} = 0, \quad v = 0, \quad \frac{\partial \theta_f}{\partial x} = 0 && \text{on } x = \frac{L}{H}, \quad 0 \leqslant y \leqslant 1,\\
&u = v = 0, \quad \frac{\partial \theta_f}{\partial y} = 0 && \text{on } 0 \leqslant x \leqslant \frac{L}{H}, \quad y = 0,\\
&\frac{\partial u}{\partial y} = \frac{\partial v}{\partial y} = \frac{\partial \theta_f}{\partial y} = 0 && \text{on } 0 \leqslant x \leqslant \frac{L}{H}, \quad y = 1,
\end{aligned} \tag{8}$$

where L is the horizontal length of the computational domain, which is chosen to be long enough compared to H to make sure that the assumption of an open boundary on the right side of the computational domain is justified.

2.2. Scaling relations

The scaling analysis is limited to the boundary layer on the isothermal vertical plate. In this region, the scales for the non-dimensionalized boundary layer thickness, vertical velocity and time at height y are defined as $\delta_b(y), v_b(y)$ and $\tau_b(y)$, respectively. It is further assumed that $v_b(y) \gg u_b(y)$ and $\delta_b(y) \ll y_s$, where $u_b(y)$ is the horizontal velocity scale at height y and $y_s = (0.5 + \theta_w/s)$ is the termination height at which the initial temperature of the local ambient equals that on the vertical plate, and thus it is the position initially having zero buoyancy. The analysis follows the same procedure used by Patterson and Imberger [4].

The analysis is firstly limited to the region $0 \leqslant y \leqslant y_s$. After that, it will be extended to the remaining region $y_s < y \leqslant 1.0$.

Balancing the unsteady and diffusion terms in (5) over the thermal boundary layer thickness $O(\delta_{b,t})$ gives

$$\delta_{b,t}(\tau) \sim Ra^{-1/4}\tau^{1/2}. \tag{9}$$

For $Pr > 1$ the buoyancy force is balanced by the viscous force in (4) yielding a transient vertical velocity scale at time τ

$$v_{b,t}(\tau) \sim Ra^{1/2}\Delta\theta_f(y)[\delta_{b,t}(\tau)]^2 \sim \Delta\theta_f(y)\tau, \tag{10}$$

where $\Delta\theta_f(y) = \theta_w - \theta_a(y) = \theta_w - (y - 0.5)s$.

Heat is also being convected vertically by the velocity (10) and the layer will continue to grow until the heat conducted in from the boundary balances that convected away.

Using (9) and (10) the balance between the convection and the conduction terms yields a growth time-scale for the full development of the thermal boundary layer at height y in the region $0 \leqslant y \leqslant y_s$,

$$\tau_{b,s}(y) \sim \left[\frac{\Delta\theta_f(y)}{y} + s\right]^{-1/2} \sim (1 + 0.5s)^{-1/2} y^{1/2} \tag{11}$$

at which time the steady-state velocity and length scales at height y have become

$$\begin{aligned}
v_{b,s}(y) &\sim \Delta\theta_f(y)\left[\frac{\Delta\theta_f(y)}{y} + s\right]^{-1/2}\\
&\sim (1 + 0.5s)^{-1/2} y^{1/2}[1 - (y - 0.5)s],
\end{aligned} \tag{12}$$

and

$$\begin{aligned}
\delta_{b,s}(y) &\sim Ra^{-1/4}\left[\frac{\Delta\theta_f(y)}{y_s} + s\right]^{-1/4}\\
&\sim Ra^{-1/4}(1 + 0.5s)^{-1/4} y^{1/4},
\end{aligned} \tag{13}$$

where $\theta_w = 1$ is assumed.

Thus the thermal layer grows until it has reached a thickness $\delta_{b,s}(y)$ in time $\tau_{b,s}(y)$. For $Pr > 1$ the diffusion of momentum maintains a velocity boundary layer, $O(\delta_{v,s}(y))$, which is thicker than the thermal boundary layer, where

$$\delta_{v,s}(y) \sim Pr^{1/2} Ra^{-1/4}\tau^{1/2} \sim Pr^{1/2}\delta_{b,s}(y), \tag{14}$$

the result given by Schlichting [5] and Patterson and Imberger [4] for natural convection flow in a homogeneous ambient fluid with differentially heated end walls.

The assumption that the boundary-layer length scales are very much less than the scale of the cavity ($\delta_{v,s}(y) \ll y_s$, that is $\delta_{v,s}(y) \ll 1$) yields the criterion

$$Ra > Pr^2, \tag{15}$$

which was given by Patterson and Imberger [4] for natural convection flow in a homogeneous environment with differentially heated end walls.

When y is in the range $y_s < y \leqslant 1.0$, heat is transferred out of the environment due to the higher temperature

there compared to that on the vertical plate. It is expected that the flow patterns within the boundary layer in this region are approximately symmetric about the horizontal plane at $y = y_s$ to those in the region $2/s \leqslant y \leqslant y_s$ and therefore the scalings (11)–(13) are also valid but y in these equations should be replaced by $(2y_s - y) = (1 + 2/s - y)$.

When $s = 0$, that is the environment is homogeneous, the scaling relations (11)–(13) become

$$\tau_b(y) \sim y^{1/2}, \quad v_b(y) \sim y^{1/2}, \quad \delta_b(y) \sim Ra^{-1/4} y^{1/4},$$

which are exactly the scaling relations obtained by Lin and Armfield [6] for the full development of the thermal

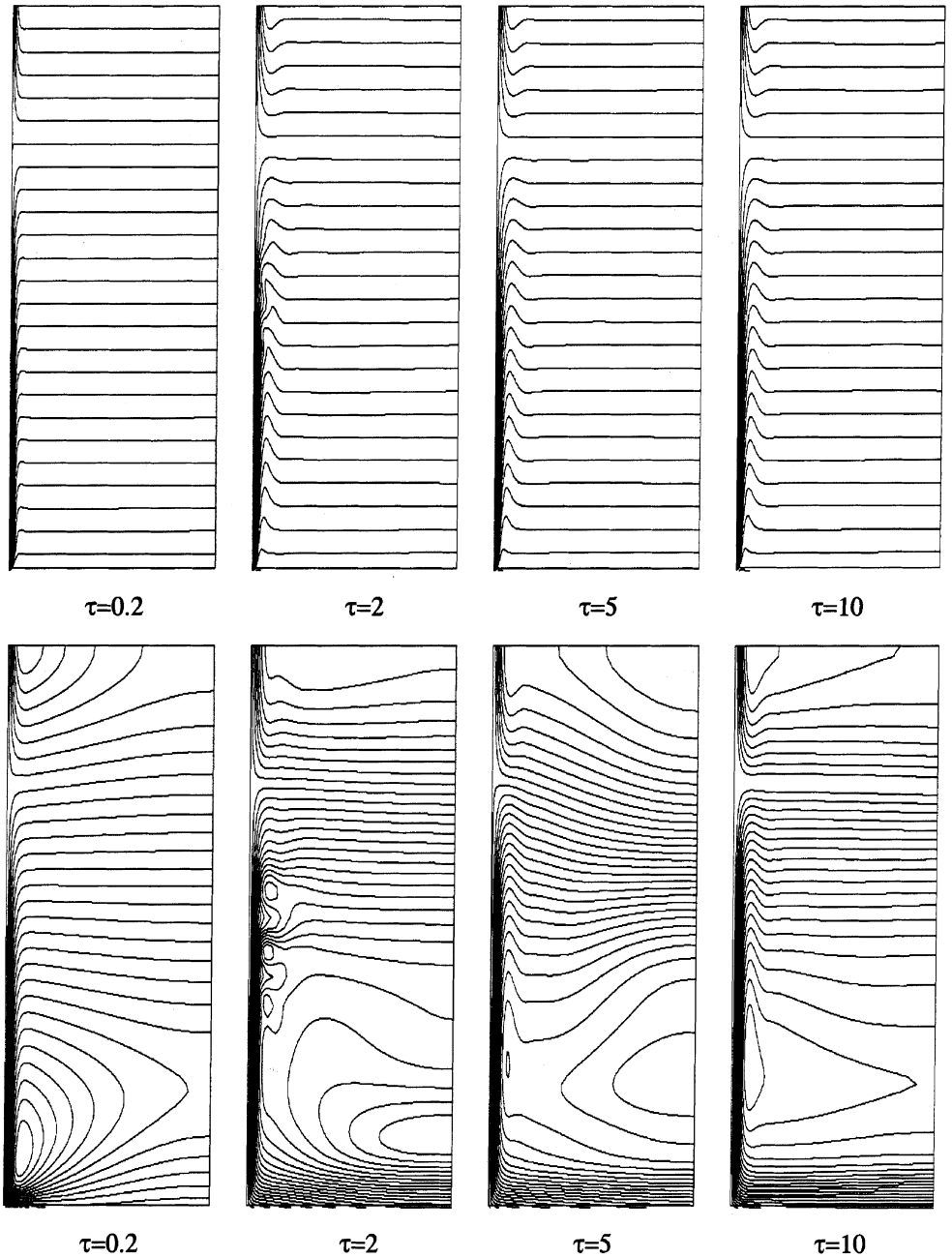

Fig. 2. Transient temperature and streamfunction contours for $Ra = 5 \times 10^8$, $Pr = 7$, and $s = 4$.

boundary layer of natural convection flow in a homogeneous fluid in a cavity.

It is noted that in the region $0 \leqslant y \leqslant y_s$ heat is conducted into the ambient while in the region $y_s \leqslant y \leqslant 1$ the situation is just the opposite. Thus, due to the approximate symmetry at $y = y_s$ the net heat transfer in the upper region of $2/s \leqslant y \leqslant 1$ is approximately zero and the mean Nusselt number $\overline{Nu}$ over the vertical plate is

$$\overline{Nu} = \int_0^{2/s} \frac{\partial \theta_f(y)}{\partial x}\,dy = \int_0^{2/s} \frac{\Delta\theta_f(y)}{\delta_b(y)}\,dy. \tag{16}$$

The evolution of the boundary-layer flow may be divided into the developing stage and the fully developed stage, as there are different scaling relations for $\delta_b(y)$ in these respective stages, that is (9) for the developing stage and (13) for the fully developed stage.

During the developing stage, the mean Nusselt number on the vertical plate is

$$\begin{aligned}\overline{Nu}(\tau) &= \int_0^{2/s} \frac{\Delta\theta_f(y)}{\delta_{b,t}(y)}\,dy \\ &= \int_0^{2/s} \frac{[1-(y-0.5)s]}{Ra^{-1/4}\tau^{1/2}}\,dy \sim \frac{Ra^{1/4}}{\tau^{1/2}}.\end{aligned} \tag{17}$$

While during the fully developed stage, it becomes

$$\begin{aligned}\overline{Nu} &= \int_0^{2/s} \frac{\Delta\theta_f(y)}{\delta_{b,s}(y)}\,dy \\ &\sim Ra^{1/4}(1+0.5s)^{1/4}\int_0^{2/s}[1-(y-0.5)s]y^{-1/4}\,dy \\ &\sim f(s)Ra^{1/4},\end{aligned} \tag{18}$$

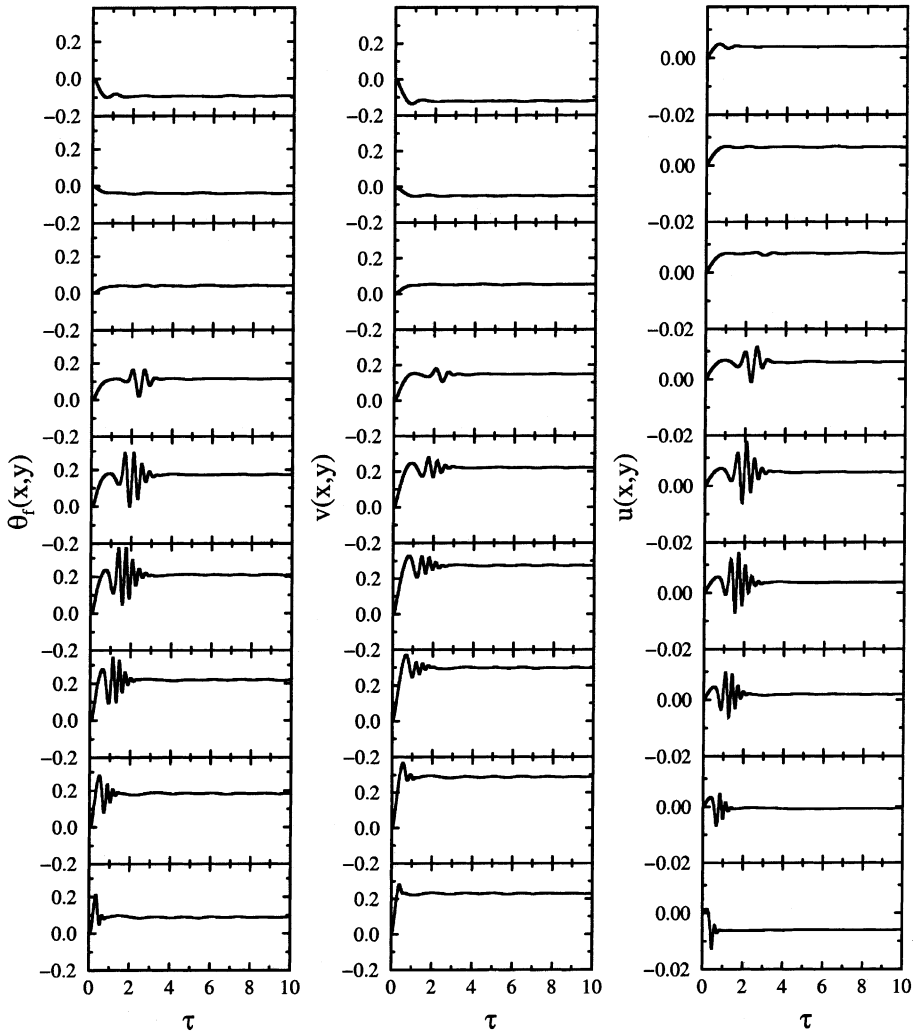

Fig. 3. Time series of $\theta_f(x,y)$, $v(x,y)$ and $u(x,y)$ at nine points inside the boundary layer for $Ra = 5 \times 10^8$, $Pr = 7$ and $s = 4.0$. All the points are located at $x = 1/120$ while from the bottom to the top $y = 0.1, 0.2, \ldots, 0.9$.

where $f(s)$ is calculated as follows:

$$f(s) = \frac{2^{11/4}}{21}(1+0.5s)^{1/4}(1+3.5s)s^{-3/4}, \tag{19}$$

which, for $2 \leqslant s \leqslant 6$, has an approximately linear relation with s. Hence, the scaling relation in (18) may be approximated by

$$\overline{Nu} \sim sRa^{1/4}. \tag{20}$$

3. Numerical results

To validate the scaling relations obtained above, direct numerical simulations have been carried out for the natural convection boundary-layer flow along a vertical isothermal plate immersed in a linearly stratified fluid with $10^6 \leqslant Ra \leqslant 10^9$, $1 \leqslant Pr \leqslant 100$, and $0 \leqslant s \leqslant 6$.

3.1. Numerical method

The governing equations (2)–(5) have been solved using a fractional-step Navier–Stokes solver [7,8]. A stretched computational mesh is used allowing grid nodes to be concentrated in regions of rapid solution variation, adjacent to the vertical plate and the upper and lower boundaries. The origin lies at the bottom left corner of the domain with y increasing up the vertical plate and x increasing horizontally into the domain, as shown in Fig. 1. The horizontal mesh size adjacent to the vertical plate is $\Delta x = 2 \times 10^{-4}$ with a grid stretching factor of 1.06 per cell until $x = 0.1$, after which the stretching factor is gradually reduced until the grid be-

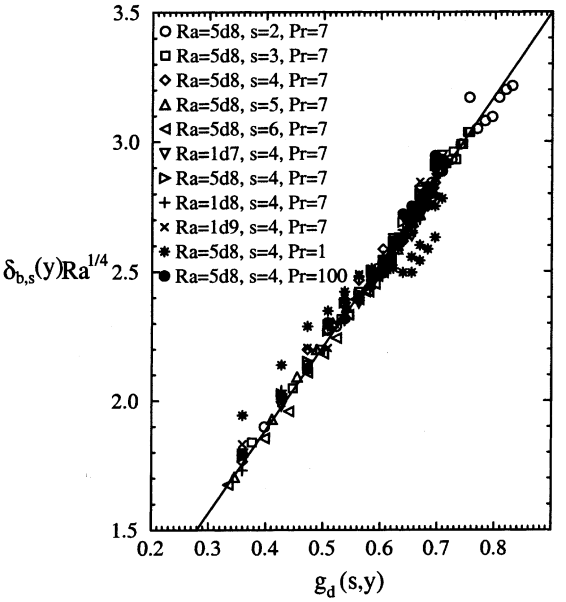

Fig. 5. $\delta_{b,s}(y)Ra^{1/4}$ plotted against $g_d(s,y)$, where $g_d(s,y) = (1+0.5s)^{-1/4}y^{1/4}$ for $0 \leqslant y \leqslant y_s$ and $g_d(s,y) = (1+0.5s)^{-1/4}(1+2/s-y)^{1/4}$ for $y_s \leqslant y \leqslant 1$.

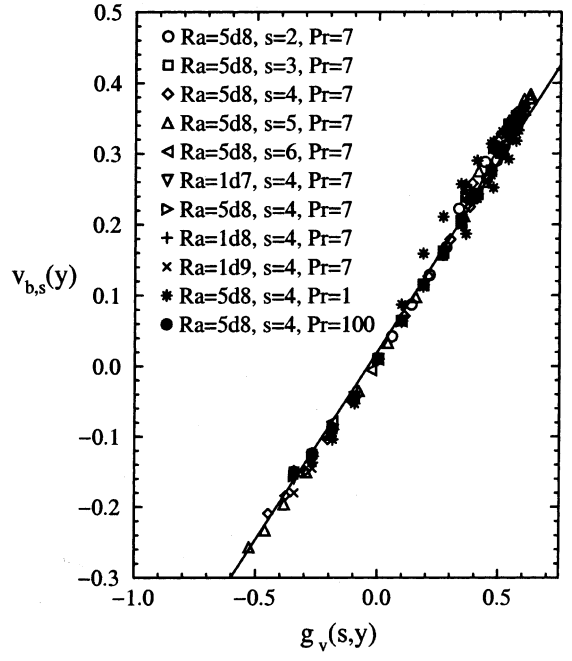

Fig. 4. $v_{b,s}(y)$ plotted against $g_v(s,y)$, where $g_v(s,y) = (1+0.5s)^{-1/2}y^{1/2}[1-(y-0.5)s]$ for $0 \leqslant y \leqslant y_s$ and $g_v(s,y) = (1+0.5s)^{-1/2}(1+2/s-y)^{1/2}[1-(0.5+2/s-y)s]$ for $y_s \leqslant y \leqslant 1$.

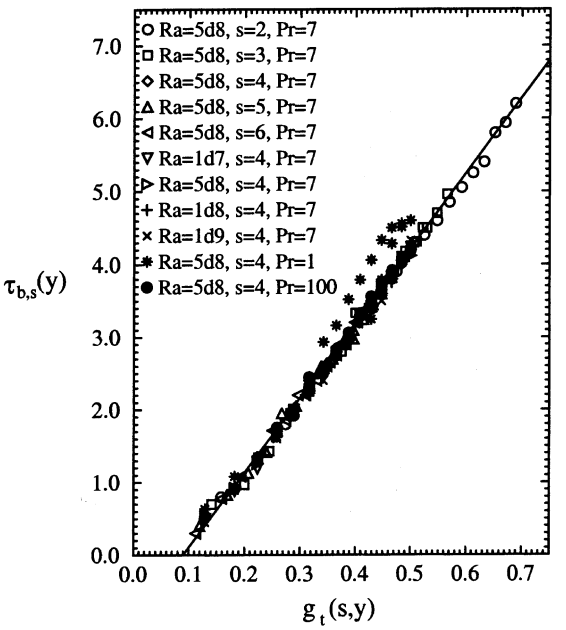

Fig. 6. $\tau_{b,s}(y)$ plotted against $g_t(s,y)$, where $g_t(s,y) = (1+0.5s)^{-1/2}y^{1/2}$ for $0 \leqslant y \leqslant y_s$ and $g_t(s,y) = (1+0.5s)^{-1/2}(1+2/s-y)^{1/2}$ for $y_s \leqslant y \leqslant 1$.

comes uniform in the interior. The vertical mesh size adjacent to the upper and lower boundaries is $\Delta y = 2 \times 10^{-3}$ with again a grid-stretching factor of 1.06 per cell until $y = 0.2$ for the lower domain and $y = 0.8$ for the upper domain, after which the stretching factor is gradually reduced until the grid becomes uniform in the interior, resulting in a mesh of 64×94 grid nodes, which are distributed symmetrically with respect to the domain half-height. The time-step used is $\Delta\tau = 1 \times 10^{-4}$.

Time-step dependency tests have been carried out by obtaining additional results at half the time-step given above. The variation in the flow patterns has been found negligible. Mesh dependency tests have also been carried out by halving the mesh size at the vertical plate and upper and lower boundaries and the stretching factor and halving the time-step. Again the solutions on the two meshes have shown negligible variation in the flow patterns.

3.2. Typical evolution of transient flow patterns

Visualizations of the evolution of the numerically simulated transient temperature and stream function contours are presented in Fig. 2 for $Ra = 5 \times 10^8$, $Pr = 7$ and $s = 4$, in this case $y_s = 0.75$. From these figures, it is seen that after the natural convection boundary-layer flow is initiated, the boundary layer at each height grows for a period of time, but with a vertical variation, as

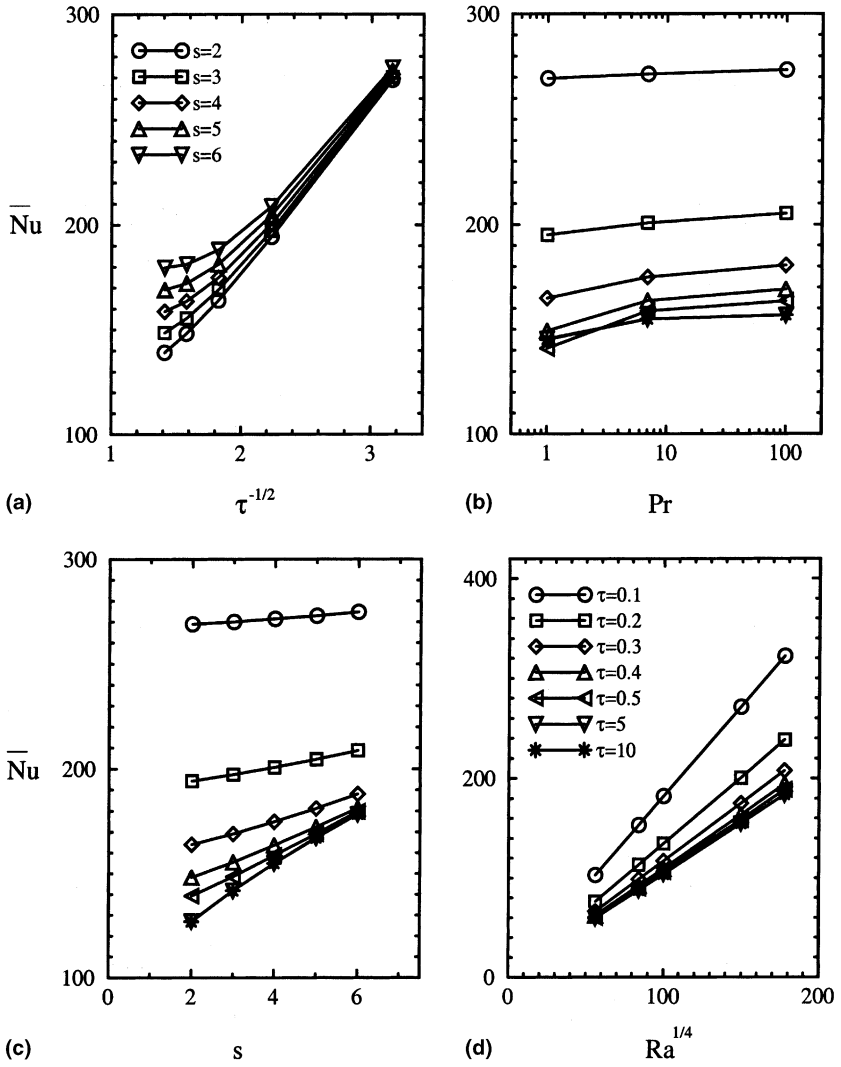

Fig. 7. $\overline{Nu}$ plotted against: (a) $\tau^{-1/2}$ for $Ra = 5 \times 10^8$ and $Pr = 7$ with five values of s; (b) Pr for $Ra = 5 \times 10^8$ and $s = 4$ at 7 times; (c) s for $Ra = 5 \times 10^8$ and $Pr = 7$ at 7 times; (d) $Ra^{1/4}$ for $s = 4$ and $Pr = 7$ at 7 times. The symbol legends in (b) and (c) are the same as those used in (d).

more clearly illustrated in Fig. 3 where the times series of $\theta_f(x,y)$, $u(x,y)$ and $v(x,y)$ at nine points within the boundary layer are presented for $Ra = 5 \times 10^8$, $Pr = 7$ and $s = 4.0$, and therefore this initial heat diffusion dominated flow is in fact two-dimensional, with the vertical variation caused by the stratification of the ambient. For the flows with homogeneous ambient, the initial heat diffusion dominated flow is one-dimensional, with no vertical variation.

At each vertical height y, the growth of the thermal boundary layer ceases with the arrival of a signal travelling up the plate from $y = 0$ in the region of $0 \leqslant y \leqslant y_s$, while travelling down the plate in the region of $y_s \leqslant y \leqslant 1$, following the signal is a series of travelling waves. The behaviour and the characteristics of these travelling waves have been extensively investigated, most of them in the context of a homogeneous ambient [9–13].

After the passing of the travelling waves, the boundary-layer flow transits to an ultimately steady flow. At $y = y_s$, the rising vertical boundary layer for $y \leqslant y_s$ ceases, ejecting an intrusion into the domain interior, while for $y \geqslant y_s$ a second boundary layer is formed travelling down the wall, which is now cooled with respect to the local ambient, also ejecting an intrusion into the domain interior. The difference in top and bottom boundary conditions means that the upper boundary layer is not an exact image of the lower, however the general structure is similar. The numerical results for other values of Ra and s show that the basic structure of the flow does not vary with Ra, although it is found that the boundary layer thickness decreases with increasing Ra, as obtained in the scaling analysis.

3.3. Numerical validation and quantification of scalings

The direct numerical simulation results used to validate the scaling relations (11)–(13) are presented in Figs. 4–6, where the maximum velocity within the boundary layer at each vertical location is used as the velocity scale and the time-scale is determined as the time when the temperature traces at each vertical location cease to change. For each combination of Ra, s and Pr results are presented at 9 locations equally spaced in the range $0 \leqslant y \leqslant 1.0$. From these figures, it is seen that the scaling results are in very good agreement with the numerical results, except the results for $Pr = 1$ where large discrepancies are observed in these figures.

Fig. 7 presents $\overline{Nu}$ plotted against $\tau^{-1/2}$, Pr, s, and $Ra^{1/4}$ for different combinations of Ra, Pr, s and τ, where $\overline{Nu}$ was obtained from the simulation by integrating the heat transfer on the plate over the full plate height. It is seen that during the developing stage of the boundary layer, $\overline{Nu}$ has approximately linear relations with $\tau^{-1/2}$ and $Ra^{1/4}$ and has little dependency on s and Pr, while after the development of the boundary layer, it shows little dependency on τ and Pr but has approximately linear relations with s and $Ra^{1/4}$, confirming the scaling relations (17) and (20). Fig. 8 shows $\bar{N}uRa^{-1/4}$ plotted against s for different values of Ra and Pr when the flows are at steady state (at $\tau = 10$), confirming again the scaling relation (20). It is noted again that the scaling predictions for $\bar{N}u$ are in very good agreement with the numerical results, except the result for $Pr = 1$ where large discrepancies are observed in the figures.

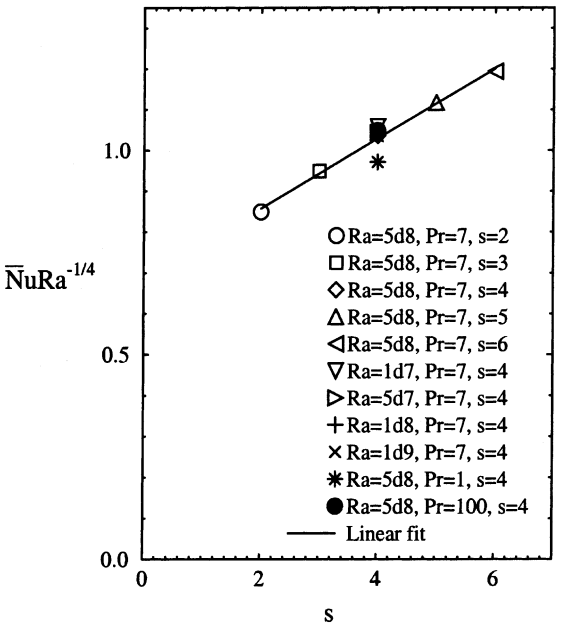

Fig. 8. $\overline{Nu}Ra^{-1/4}$ plotted against s for different values of Ra and Pr when the flows are at steady state (at $\tau = 10$).

The scaling analysis in Section 2.2 is only for $Pr > 1$. When $Pr \to 1$, it is found that the numerical results begin to deviate considerably from the scaling relations (11), (12), (13), (17) and (20). The reason for these deviations is that when $Pr \sim 1$, the unsteady inertia force, the viscous force and the buoyancy force are at the same order and it is impossible to only use the balance between the buoyancy and viscous forces to yield the transient vertical velocity scale at time τ, as was used to obtain (10) for $Pr > 1$. It is therefore impossible to obtain scaling relations similar to (11), (12), (13), (17) and (20) for $Pr \sim 1$.

Acknowledgements

The financial support of an AusAID scholarship and from the National Natural Science Foundation and Yunnan Province of P.R. China to W. Lin and the Australian Research Council are gratefully acknowledged.

References

[1] Y. Joshi, B. Gebhart, Transient response of a steady vertical flow subject to a change in surface heating rate, Int. J. Heat Mass Transfer 31 (1988) 743–757.
[2] Y. Jaluria, B. Gebhart, Stability and transition of buoyancy-induced flows in a stratified medium, J. Fluid Mech. 66 (1973) 593–612.
[3] R.A.W.M. Henkes, C.J. Hoogendoorn, Laminar natural convection boundary-layer flow along a heated vertical plate in a stratified environment, Int. J. Heat Mass Transfer 32 (1988) 147–155.
[4] J.C. Patterson, J. Imberger, Unsteady natural convection in a rectangular cavity, J. Fluid Mech. 100 (1980) 65–86.
[5] H. Schlichting, Boundary-layer Theory, seventh ed., McGraw-Hill, New York, 1979.
[6] W. Lin, S.W. Armfield, Direct simulation of natural convection cooling in a vertical circular cylinder, Int. J. Heat Mass Transfer 42 (1999) 4117–4130.
[7] S.W. Armfield, R. Street, The fractional-step method for the Navier–Stokes equations on staggered grids: the accuracy of three variations, J. Comput. Phys. 153 (1999) 660–665.
[8] W. Lin, S.W. Armfield, Direct simulation of weak axisymmetric fountains in a homogeneous fluid, J. Fluid Mech. 403 (2000) 67–88.
[9] S. Ostrach, Laminar Flows with Body Forces, Oxford University Press, Oxford, 1964.
[10] R.J. Goldstein, D.G. Briggs, Transient free convection about vertical plates and circular cylinders, ASME J. Heat Transfer 86 (1964) 490–500.
[11] S.N. Brown, N. Riley, Flow past a suddenly heated vertical plate, J. Fluid Mech. 59 (1973) 225–237.
[12] B. Gebhart, R.L. Mahajan, Instability and transition in buoyancy induced flows, Adv. Appl Mech. 22 (1982) 231–315.
[13] S.W. Armfield, J.C. Patterson, Wave properties of natural-convection boundary layers, J. Fluid Mech. 239 (1992) 195–211.